

THE OCCURRENCE OF A SUBUNIT  
PATTERN IN THE UNIT MEMBRANES  
OF CLUB ENDINGS IN MAUTHNER CELL  
SYNAPSES IN GOLDFISH BRAINS

J. DAVID ROBERTSON, M.D.

From the Department of Neurology and Psychiatry, Harvard Medical School, Boston, and the Research Laboratory, McLean Hospital, Belmont, Massachusetts

ABSTRACT

Observations additional to those previously reported (34) on boutons terminaux and club endings on Mauthner cell lateral dendrites, primarily as seen in sections of permanganate-fixed material, are described. Certain new findings on  $\text{OsO}_4$ -fixed endings are also included. The boutons terminaux are closely packed in the synaptic bed with  $\sim 100$  to  $150$  A gaps between their contiguous unit membranes and a few interspersed glial extensions. Their synaptic membrane complexes (SMC) appear as pairs of unit membranes separated by  $\sim 100$  to  $150$  A clefts. They contain many vesicles and unoriented mitochondria, but no neurofilaments. The club endings after  $\text{KMnO}_4$  fixation are, as after  $\text{OsO}_4$  fixation (34), again seen surrounded by a layer of extracellular matrix material. These endings contain relatively few synaptic vesicles, a few unit membrane limited tubules  $\sim 300$  A in diameter, and mitochondria oriented perpendicular to the SMC. Neurotubules and neurofilaments are not clearly seen. These components are also virtually absent in the Mauthner cytoplasm. No ribosomes are seen in the  $\text{KMnO}_4$ -fixed material. The unit membranes of the SMC of club endings show up clearly in essentially the same junctional relations described after formalin- $\text{OsO}_4$  fixation (34). In addition, the synaptic discs in transverse section show a central beading repeating at a period of  $\sim 85$  A associated with scalloping of the cytoplasmic surfaces. In oblique views, dense lines are seen repeating at a period of  $\sim 90$  A. In frontal views a hexagonal array of close-packed polygonal facets is seen. These repeat at a period of  $\sim 95$  A. Each has a central dense spot  $< 25$  A in diameter. Similar subunits are seen in the unit membranes of synaptic vesicles.

INTRODUCTION

A separate report (34) presents a description of certain Mauthner cell synapses in goldfish brains studied after fixation with  $\text{OsO}_4$  and formalin- $\text{OsO}_4$ . The present paper presents new findings in these synapses primarily in material fixed with potassium permanganate but with additional observations on  $\text{OsO}_4$ -fixed material related to the new findings in the  $\text{KMnO}_4$ -fixed material. It is concerned mainly with the observation

of a characteristic subunit pattern of the unit membranes in the synaptic discs (34) of club endings. The findings have been reported in preliminary form (32).<sup>1</sup>

---

<sup>1</sup> The micrographs were first shown as an addition to a paper and demonstration at the San Francisco meeting of the Society for Cell Biology (33) in November, 1962.

## MATERIALS AND METHOD

Common goldfish (*Carassius auratus*), 2 to 4 inches in length, as described in the previous paper (34), were used throughout.

The brains were fixed by a modification of the perfusion technique of Palay *et al.* (21). This technique works well for OsO<sub>4</sub> fixation but it has not been successful in our hands for good permanganate fixation. Several modifications have been tried in attempting to get good specimens with permanganate with only sporadic success. The technique that follows was used for the specimens illustrated.

The goldfish is anesthetized by immersion in crushed ice in water until swimming motions cease. It is then packed in crushed ice and the heart exposed. 0.25 ml of Panheprin (Abbott Laboratories, North Chicago; 10,000 u.s.p. units per ml) is injected with a No. 27 needle into the ventricle. The conus arteriosus is incised and a small Intramedic polyethylene tube, PE 10, (Clay-Adams Inc., New York) is inserted into the aorta and tied in place. The tube has been previously connected to a hypodermic needle attached to a 2 ml syringe filled with 0.7 per cent sodium nitrite. One to 1.5 ml of this solution is injected carefully. In small fish this frees the gills of blood and no further flushing with Ringer solution is necessary. The syringe is then replaced, taking care not to introduce air bubbles, with a 10 ml syringe completely filled with a 1.5 per cent permanganate fixing solution of the following composition: NaCl, 0.30 gm/liter; KCl, 0.19 gm/liter; CaCl<sub>2</sub>, 0.17 gm/liter; NaHCO<sub>3</sub>, 15.00 gm/liter; pH 7.4. The first 10 ml of fixative is kept at room temperature and injected rapidly (10 ml in about 30 to 40 seconds taking care not to rupture small vessels). The syringe is then refilled with fixative, replaced, taking care not to introduce air bubbles, and the injection continued. The fixative in the second and subsequent syringes is chilled to ice water temperature. Six or eight successive injections are made until 60 to 80 ml of fixative has been used. The medulla is then dissected out and sliced transversely into pieces 0.5 to 1.0 mm thick in cold Ringer solution. The slices are then placed in Minicube ice cube trays in ice cold fixative for the balance of 4 hours. They are dehydrated and embedded in Araldite by the method given in the previous paper (34). The Mauthner cell is located by the method previously outlined.

We have found it quite difficult to obtain well fixed preparations consistently with permanganate. Despite some successes with the above technique our results were quite erratic. It is easier to obtain apparently well fixed material if the animal and all perfusing fluids are kept at room temperature but these preparations have been disappointing in electron micrographs. We believe that chilling the animal or the fixative or both is necessary for good quality fixation

of this material. It is this, however, that causes difficulty.

We believe that the critical factors in obtaining successful results are, the use of a higher (1.5 per cent) concentration of permanganate in suitable salts, the chilling procedures, and the rate at which the injections are carried out. It is possible to judge very quickly whether or not successful perfusion has been achieved by sectioning the medulla immediately after the injections have been completed. Only those specimens that are uniformly darkened through the entire sections are worth further study.

The OsO<sub>4</sub>-fixed specimens were prepared according to the method described in the previous paper (34) using the 2.5 per cent OsO<sub>4</sub> fixative. After dehydration in acetone the specimens were immersed in 1 per cent KMnO<sub>4</sub> in acetone for 15 minutes and then washed twice briefly in acetone containing two drops of methyl acrylate per 25 ml (Eastman Organic Chemicals, Rochester, New York, containing hydroquinone inhibitor) according to the method of Parsons (22).

Sections for electron microscopy were cut with a Dupont diamond knife in an LKB microtome and collected on Athene slit grids of an original design covered by carbon films. The permanganate-fixed specimens were examined unstained but the OsO<sub>4</sub>-fixed specimens were stained with lead by Karnovsky's method A (19). A Siemens Elmiskop 1 b electron microscope was used equipped with molybdenum apertures. A mechanically pointed filament sharpened after Bradley's technique (2) was used.<sup>2</sup> A 100  $\mu$  condenser aperture and a 50  $\mu$  objective aperture were used for most observations. Condenser I was set at + 17 controller steps and either 80 or 100 kv was generally used although some micrographs were taken at 40 kv in an unsuccessful effort to improve contrast. A fixed 300  $\mu$  platinum objective centering aperture was used since this reduced contamination of the externally centerable objective aperture. A Wray Optical Company (London, England) stereomicroscope giving 10 X was used throughout. The beam current was kept below 10  $\mu$ amps and most often well below 5  $\mu$ amps. Under these conditions illumination was adequate to electronic magnifications in excess of 100,000.

The standard Siemens low temperature stage adjusted to the temperature giving zero contamination was used for some observations. The absence of contamination was helpful but there was no other appreciable effect on the image.

<sup>2</sup> Mr. C. W. French of 15 Peterson Road, Natick, Mass. prepared the filaments from the standard Siemens filaments by his own modification of the Bradley technique, following suggestions by Dr. J. B. Caulfield.

Figs. 6, 10, and 11 are from  $\text{OsO}_4$ -fixed material stained by Parson's permanganate technique (22) before embedding and by Karnovsky's lead method A after sectioning. All other micrographs are of material fixed with  $\text{KMnO}_4$  and unstained.

A Joyce-Loebl microdensitometer was used for the text figures. It was used at an optical magnification of  $\times 10$ , a record speed of 5, and sensitivity of 6, with a 0.39 D gray wedge. The lever ratios and slit widths are given in the figure legends.

## RESULTS

### A. Boutons Terminaux

Fig. 1 shows a group of boutons terminaux (*b*) on a Mauthner cell lateral dendrite (*M*) fixed with  $\text{KMnO}_4$ . Note the closely investing clear glia cell extensions (*g*) and the nearby capillary (*C*) with its endothelial cell (*E*) separated from the glia by a gap  $\sim 500$  Å wide. There are cellular profiles (*x*) that lie beneath the endothelial cells separated from them by a gap  $\sim 100$  to 150 Å wide and from the adjacent glia cells by the same  $\sim 500$  Å gap between the endothelial cells and glia cells. The nature of these profiles is unknown but they may be overlapping extensions of endothelial cells. The boutons are filled by rather uniformly packed synaptic vesicles though there may be a slight preferential concentration next to the SMC in some. They contain numerous mitochondria that are cut in various orientations suggestive of a random arrangement of elongated shapes. The mitochondrial profiles are preferentially located near the sides of the boutons profiles away from the SMC. Note, within the Mauthner lateral dendrite to the left, the mitochondrion (arrow 1 and lower inset) that shows an apparent extension of its outer membrane as a tubular or cisternal form indistinguishable from endoplasmic reticulum components (30).

The pre- and postsynaptic membranes of the boutons are separated by a gap that measures by eye  $\sim 150$  to 200 Å in width (upper inset enlargement) as in the corresponding  $\text{OsO}_4$ -fixed endings. The microdensitometer tracing in Fig. 2 was made along the direction of arrow 2 in Fig. 1. It shows the density peaks in the two unit membranes of the synaptic membrane complex (SMC) and permits more objective measurements. The peak to peak separation of the limiting dense strata of one unit membrane is 45 Å and the other 49 Å. The gap width peak to peak is 170 Å and the overall SMC width peak to peak is 264 Å.

These measurements are reasonably close to the ones made by eye if one considers that in the latter measurements an average is made of the rising and falling density peaks. The densitometer method is certainly more objective but since it does not take into account variations from one region to another, measurements made in this way, without statistically significant samples, must also be considered only approximations.

In the permanganate-fixed preparations as in Fig. 1 the triple-layered unit membrane structures show up regularly. This is the most striking difference between the membranes in the  $\text{OsO}_4$ - and  $\text{KMnO}_4$ -fixed materials.  $\text{OsO}_4$  fixation only occasionally shows up the triple-layered appearance of the unit membranes. This effect was first appreciated and interpreted as a deficiency of  $\text{OsO}_4$  fixation from studies of nerve myelin (26, 28–30). The appearance of the unit membranes after permanganate fixation is accordingly taken as more representative of their native state.

### B. Club Endings

Fig. 3 shows, at low power, a club ending after fixation with permanganate and embedding in Araldite. The lateral dendrite (*M*) lies to the left. The general picture is similar to that found after  $\text{OsO}_4$  fixation. The termination of the myelin sheath is similar to that found in nodes and the bare terminal axon is again found surrounded by a layer of extracellular matrix material (\*) of varying thickness. The matrix material is considerably less dense than it is in  $\text{OsO}_4$  fixed specimens. The neurofilaments of the axoplasm of the endings are not distinguishable and it is important to note that the  $\sim 200$  Å neurotubules that are so prominent in the formalin- $\text{OsO}_4$  fixed specimens do not appear. The only tubular forms seen measure  $\sim 300$  Å in diameter and are considered components of the endoplasmic reticulum (ER) since some show clear unit membranes. The Mauthner cytoplasm displays a qualitatively similar picture. Since the neurotubules are not well fixed by  $\text{KMnO}_4$  they probably are not high in phospholipid content since  $\text{KMnO}_4$  is a good fixative for phospholipids (29, 37). Very few mitochondria or synaptic vesicles are present in this particular ending although these organelles are abundant in the adjacent boutons terminaux and occur in larger numbers in other nearby club endings.

The synaptic membrane complex (SMC) in Fig. 3 is obliquely sectioned in some places but

some of the synaptic discs that are transversely sectioned show clearly the strata expected of an external compound membrane (27) formed by contact of two unit membranes. One such disc section from another micrograph at higher magnification is shown in the inset enlargement. This should be compared with the disc from an OsO<sub>4</sub>-fixed specimen in Fig. 6. The synaptic discs are of about the same size, shape, and distribution in both permanganate- and OsO<sub>4</sub>-fixed material. The discs are believed to be formed by the intimate apposition of the presynaptic and postsynaptic unit membranes with a complete occlusion of the usual ~100 to 200 Å wide intermembrane gap. The discs are only ~0.3 to 0.5 μ in diameter and occupy only a fraction (perhaps as much as half) of the total synaptic area. In between the discs the pre- and postsynaptic membranes are separated by the usual ~100 to 200 Å intermembrane gap (see reference 34).

Portions of other synaptic discs caught in perpendicular section are enlarged in Figs. 4 and 8. The external compound membranes (ECM's) here each measure, by eye, ~125 Å in over-all thickness but in some instances measurements as high as 160 Å have been found (average of 127 Å from measurements in 13 different regions by eye). Each of the synaptic discs as seen in transverse section consists of five layers as follows: (1) a dense stratum bordering axoplasm; (2) a light zone; (3) a central dense stratum with localized bead-like thickenings; (4) a light zone; and (5) a dense stratum. These five strata are evident in Fig. 4 as well as in the microdensitometer tracing

in Fig. 5 taken across the synaptic disc in Fig. 4 along the direction of the arrow.

The beading along the central dense stratum of vertically sectioned synaptic discs as in Figs. 3, 4, and 8 repeats regularly. This is very clear in the KMnO<sub>4</sub>-fixed specimens but less so in OsO<sub>4</sub>-fixed material as in Fig. 6. Fig. 13 is a microdensitometer tracing along the length of a transversely sectioned KMnO<sub>4</sub>-fixed synaptic disc like the one in Fig. 4. The average repeat period of the beads is 85 Å (average of 86 Å in 40 measurements by eye). There is usually a suggestion of a density traversing the two light zones of each of the two unit membranes (layers 2 and 4) in association with the dense spots or beads in layer 3. This, in places, (arrows; Figs. 3, inset, and 4) seems to be associated with or due to a scallop-like indentation of the cytoplasmic dense strata opposite each of the dense central spots. Although the transverse densities are indistinct and there is no complete clear-cut interruption of the light central zones of the united unit membranes, they may prove to be a reflection of an underlying pattern of molecular organization involving the lipid cores of the membranes.

Only suggestions of such structural differentiations have so far been made out in OsO<sub>4</sub>-fixed preparations like that in Fig. 6. However, the over-all dimensions and appearances are sometimes very nearly the same. The microdensitometer tracing in Fig. 5 across the disc in Fig. 4 should be compared with the complementary tracing in the OsO<sub>4</sub>-fixed specimen in Fig. 7 taken along the direction of arrow *l* in Fig. 6. In each example three density peaks are obtained at similar

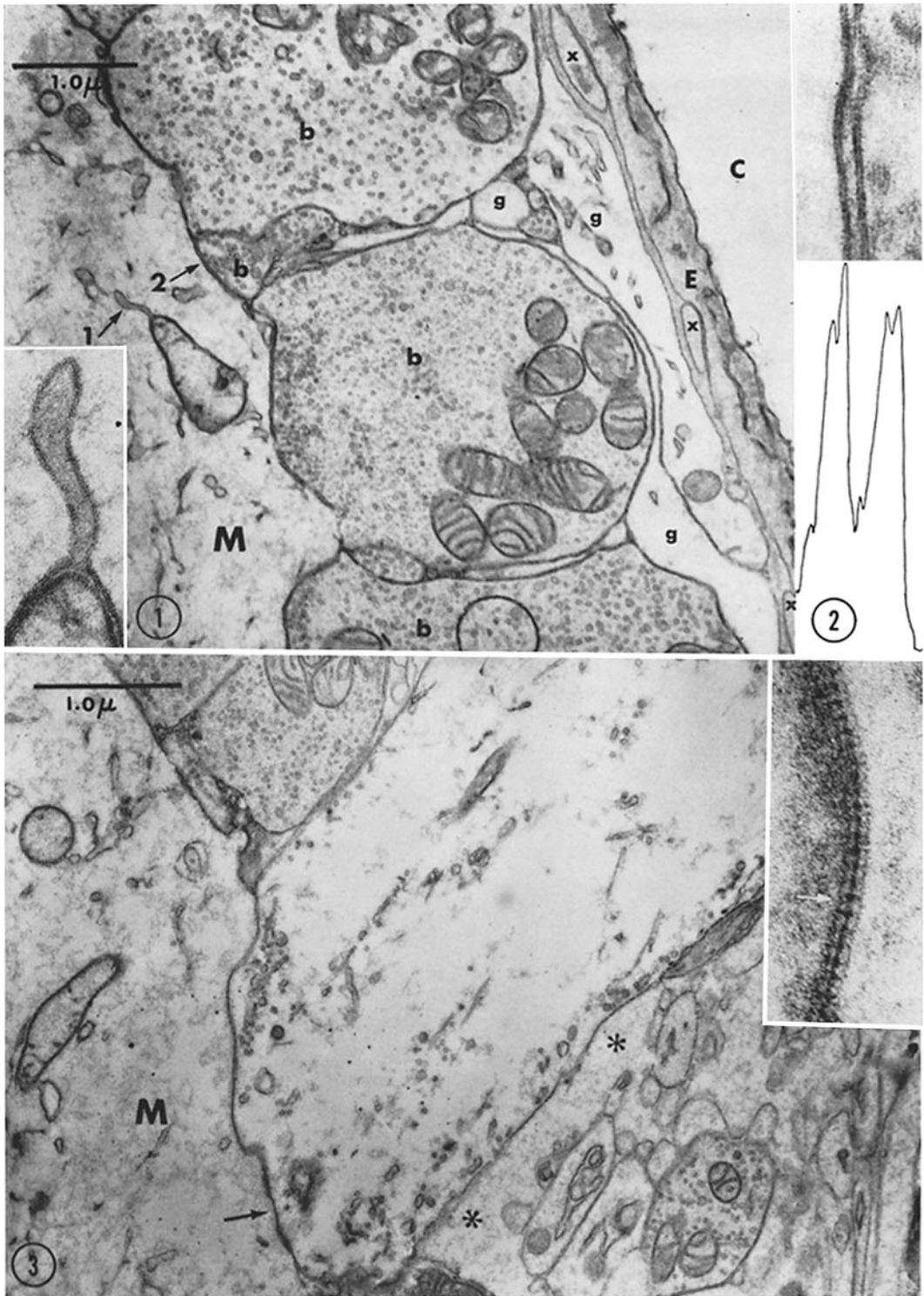
---

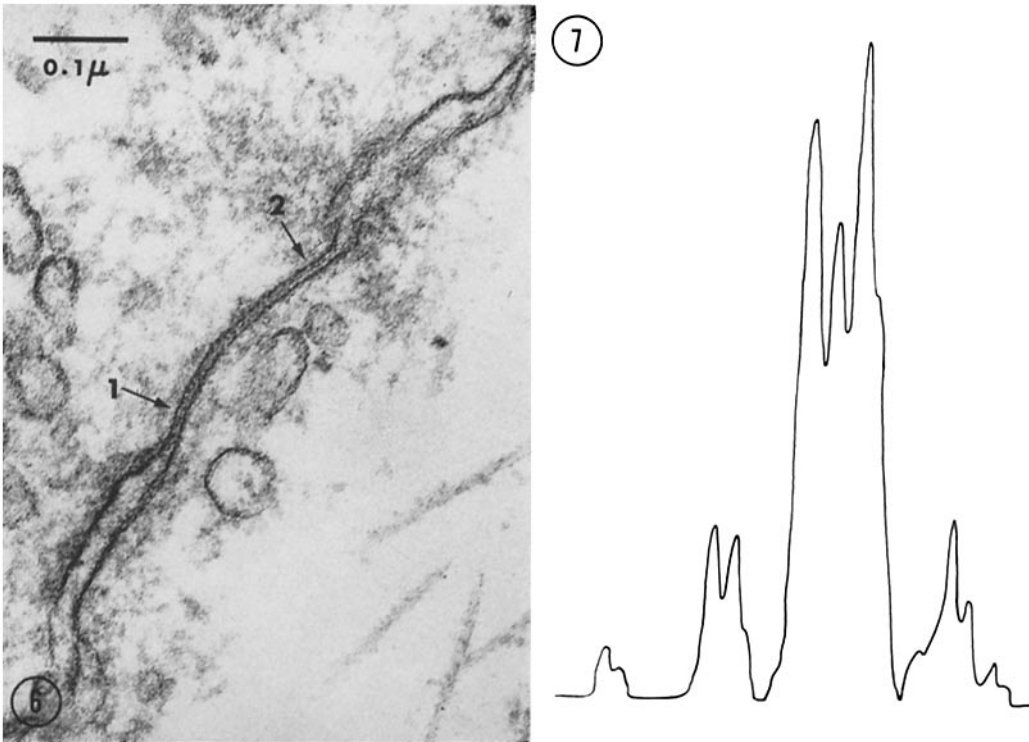
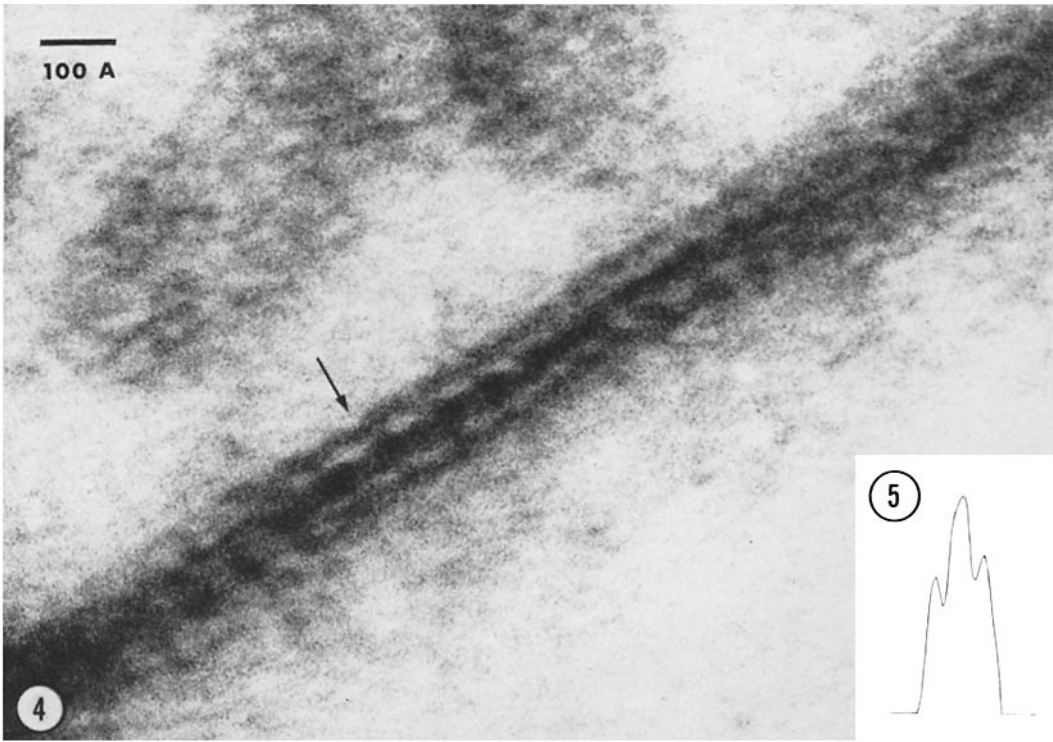
FIGURE 1 Section of bouton terminaux (*b*) on lateral dendrite of Mauthner cell (*M*). A capillary (*C*) appears to the right bounded by an endothelial cell (*E*) with unknown profiles (*X*). The endings are separated from the capillary by relatively light glia cells (*g*). Note the extension of the outer membrane of the mitochondrion at the arrow enlarged in the lower inset. A portion of the synaptic membrane complex (arrow 2) is enlarged to the upper right. × 19,000. Lower inset, × 86,000; upper inset, × 260,000.

FIGURE 2 Microdensitometer tracing across the central portion of the synaptic membrane complex in the inset enlargement to Fig. 1. Lever ratio 100:1; slit width 0.25 mm. × 390,000.

FIGURE 3 Section of club ending (*C*) on lateral dendrite of Mauthner cell (*M*). A synaptic disc like the one designated by the arrow but from another micrograph is enlarged in the inset. Note the extracellular matrix material (\*) around the ending. × 23,000; ‡ inset, × 260,000.

‡ This figure is estimated since an error was made in recording the original magnification.





spacings. The central peak approximately bisects the intervening density trough in each case. In the OsO<sub>4</sub> or formalin-OsO<sub>4</sub> fixed material reported in the previous paper the central dense stratum representing the combined outer dense strata of the two unit membranes often failed to show up. In such instances the over-all thickness of the SMC as measured by eye was between 150 and 200 Å and it seems reasonable to ascribe both the absence of the central dense stratum and the slight increase in over-all thickness to a failure of OsO<sub>4</sub> to fix the central components adequately. This viewpoint is consistent with the relatively great reduction of the central density peak in Fig. 7 as compared with Fig. 5.

The over-all thickness of the synaptic discs is of some interest since some of the measurements are considerably less than that usually found in external compound membranes. It is important to decide whether or not this decrease reflects some degree of fusion of the two constituent unit membranes (31, 35). Fusion is taken here to differ from intimate apposition in the sense that fusion implies a reduction in the total number of monomolecular layers of the two constituent unit membranes from four for each membrane to some smaller number (see reference 31). Intimate apposition implies only the close juxtaposition and perhaps some degree of overlapping and interpenetration of side chain groupings of the closely apposed outer surface monolayers of the unit membranes involved. The over-all thickness of the discs and the presence or absence of the five strata expected of a compound membrane are important in considering this question. It should be borne in mind here that the two unit membranes of mesaxons of myelinated nerve fibers when closely apposed usually measure ~150 Å across while the same membranes within compact myelin measure

100 to 130 Å in over-all thickness (the radial repeat period) depending on preparatory methods. There is evidence that this reduction is not associated with fusion as defined above since the membranes separate apparently intact in Schmidt-Lantermann clefts and after experimental modifications (27, 29). Should the minimal figures of ~125 Å for the thickness of the synaptic discs be taken as evidence of unit membrane fusion in some cases or be ascribed to differences in preparatory methods? This question cannot as yet be definitely answered.

Measurements of over-all thicknesses of membranes made by eye are subject to a considerable degree of arbitrariness. It is less arbitrary to compare the peak to peak separations in densitometer traces of the dense strata bordering the synaptic membrane complexes. The densitometer tracing in Fig. 5 across the central part of the permanganate fixed SMC in Fig. 4 shows a peak to peak separation of the bordering dense strata of 85 Å. In Fig. 7 the similar tracing across the OsO<sub>4</sub> fixed SMC in Fig. 6 near arrow 1 shows a peak to peak separation of 89 Å. The difference appears slight. However, a similar tracing made across the same SMC in Fig. 6 but near arrow 2 gave a peak to peak separation of 98 Å. This variation, although perhaps significant, probably should best be taken as an indication of the element of arbitrariness even in densitometer traces. This makes clear the need for a thorough statistical analysis if any significance is to be placed on differences in measurements such as the ones given. No such statistical study has yet been attempted. Hence in this paper no significance is assigned to such variations in SMC thickness as the ones under discussion and no definite conclusions are reached with regard to the fundamentally important question of membrane fusion. It seems justifiable to say only that the

---

FIGURE 4 Portion of a synaptic disc. Note the beading of the central dense stratum and the scalloped effect at the arrow. The presynaptic cytoplasm is above.  $\times 1,000,000$ .

FIGURE 5 Microdensitometer tracing across the central portion of the synaptic disc in Fig. 4. Lever ratio 50:1; slit width 1.0 mm.  $\times 810,000$ .

FIGURE 6 Portion of SMC of a club ending fixed with OsO<sub>4</sub> and "stained" with KMnO<sub>4</sub> and lead. The Mauthner cytoplasm lies to the lower right. See text for arrow designations.  $\times 125,000$ .

FIGURE 7 Microdensitometer tracing across the SMC in Fig. 6 near arrow 1. Lever ratio 50:1; slit width 1.0 mm.  $\times 750,000$ .

evidence is against complete fusion. Some degree of partial fusion may occur but this matter requires further study before definite conclusions can be reached.

Figs. 8 to 12 show SMC's at higher magnification that are in some regions obliquely sectioned with respect to the plane of the membranes. Figs. 8, 9, and 12 were fixed first with  $\text{KMnO}_4$ . The other two (Figs. 10 and 11) were fixed first with  $\text{OsO}_4$ . In Fig. 8 the direction of sectioning is perpendicular to the synaptic disc in the lower center and all five layers show up clearly. This disc is twisted considerably in the lower part of the section. Here one does not see the fine strata but instead sees a faint suggestion of a system of regularly repeating transverse lines. This is much more clearly shown at the top where another synaptic disc is seen tilted only slightly. A similar slightly tilted disc fixed with  $\text{OsO}_4$  is shown in Fig. 10. The transverse period in more obliquely sectioned membranes shows up better in Figs. 9, 11, and 12. Here one sees dense lines  $\sim 20$  A thick repeating at a period of  $\sim 90$  A from microdensitometer tracings such as those in Figs. 14 to 16. Fig. 14 was made along the obliquely sectioned disc nearly in the center of Fig. 9. The average spacing is 90 A (average of 42 measurements by eye in other micrographs 88 A). Figs. 15 and 16 were made along the obliquely sectioned discs enlarged in the insets above Figs. 10 and 11. Here the average periods are respectively 85 A and 90 A after  $\text{OsO}_4$  fixation. Although not shown in the densitometer traces, the light zones between each pair of thick lines in the obliquely sectioned

discs is bisected by a thinner dense line  $< 20$  A thick (arrows in lower inset Fig. 12 and arrow in upper inset Fig. 11). I shall return to these intraperiod lines further on to designate the structures responsible for them.

Fig. 12 shows in its center one synaptic disc (arrow *I*) that is oriented with its membranes very nearly parallel to the plane of the section so that it appears in a frontal view turned  $90^\circ$  from the one in Fig. 4. Here one sees a honey-comb-like hexagonal array of closely packed subunits appearing as geodesic facets each measuring roughly by eye about 90 to 100 A in over-all width (upper inset enlargement). A similar array is seen in frontal view in the disc (*d*) included in Fig. 18. The array of facets in such frontal views repeats at a period of about 95 A (average of 22 measurements by eye, 96 A). A microdensitometer trace of this repeat period in Fig. 12 is shown in Fig. 17. The average of 72 spacings in this specimen is 94 A. The differences between the repeat period in transversely ( $\sim 85$  A), obliquely ( $\sim 90$  A), and frontally ( $\sim 95$  A) viewed synaptic discs may be significant. This is being studied further and an analysis of alternative lattice models will be reported separately.

Each individual facet of the repeating subunit array appears as a light area bounded by dense straight lines  $< 20$  A thick as measured by eye arranged in a regular fashion around the border. These dense borders are shared by adjoining facets. Each facet has a dense spot in its center  $< 25$  A in diameter, again as measured by eye. In some places the subunit facets appear to have six sides

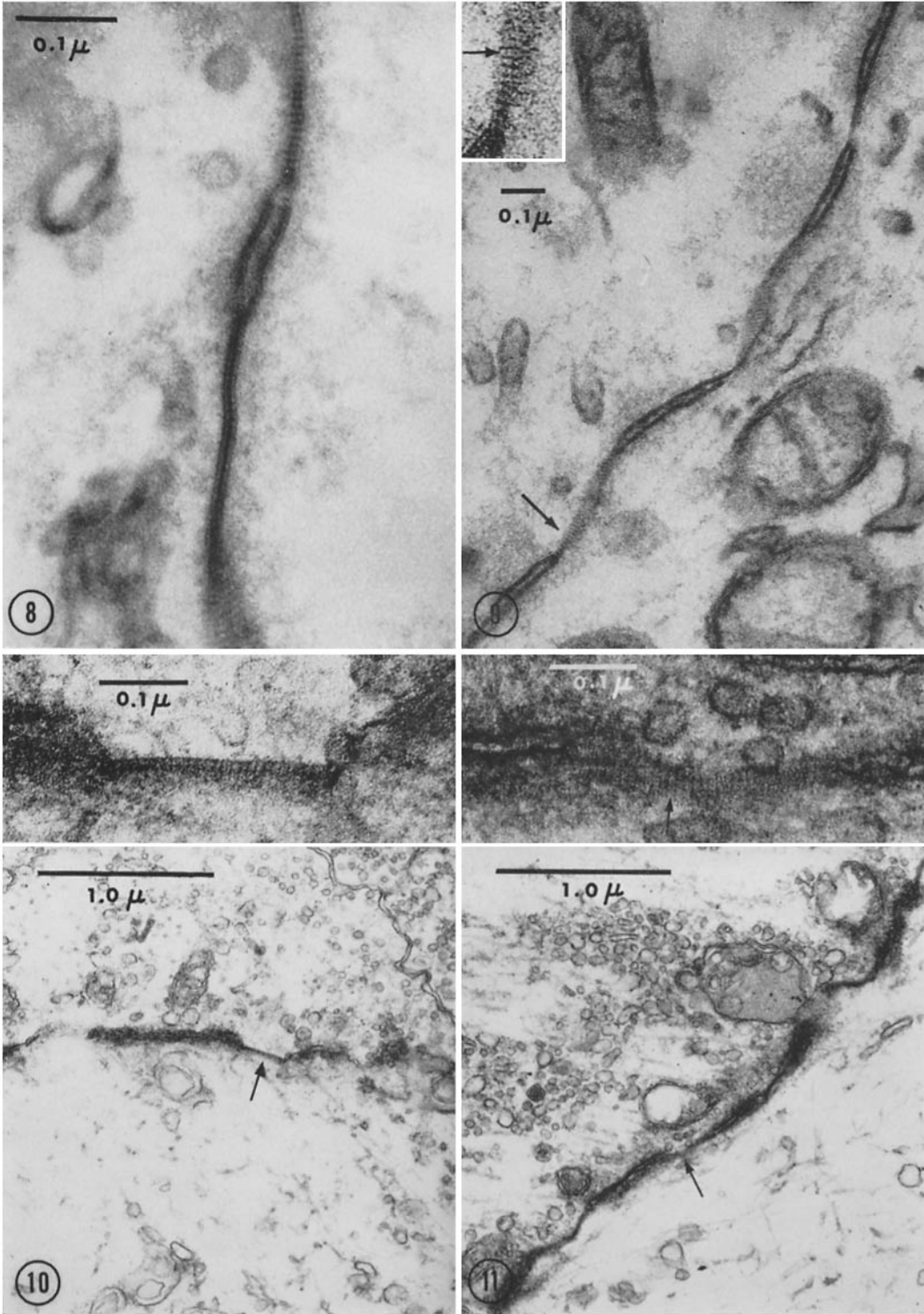
---

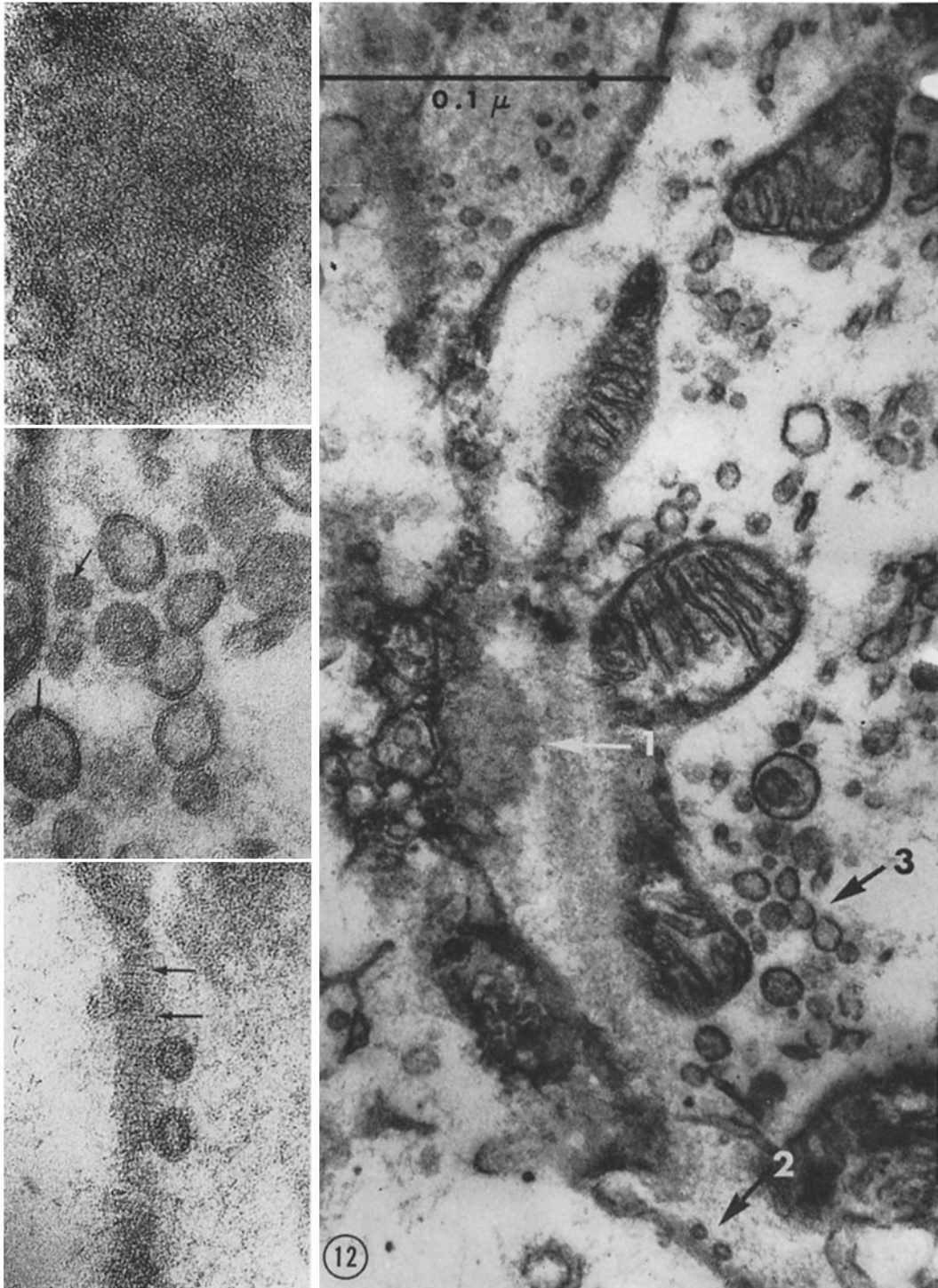
FIGURE 8 Portion of two synaptic discs with intervening region with a widened cleft. Presynaptic axoplasm to the left.  $\times 160,000$ .

FIGURE 9 Section of club ending with obliquely sectioned synaptic discs showing a regular transverse repeat period. One of these (arrow) is enlarged to the upper left. The individual subunit facets can be made out with their aligned edges making the major repeating lines and the central dots making a less conspicuous intraperiod line (inset arrow).  $\times 66,000$ ; inset  $\times 150,000$ .

FIGURE 10 Portion of the SMC of a club ending fixed with  $\text{OsO}_4$  and stained with  $\text{KMnO}_4$  and lead. One synaptic disc (arrow) is shown slightly obliquely sectioned. This is enlarged in the inset above. Note the transverse striations.  $\times 26,000$ ; inset,  $\times 130,000$ .

FIGURE 11 Section similar to Fig. 10, prepared in the same way. The SMC is more obliquely sectioned here and the disc (arrow) enlarged in the inset shows heavy dense lines repeating regularly at a period of 90 A. The space between each of the heavy lines is bisected by a row of dots forming in places an intraperiod line. One of these is designated by the arrow in the inset.  $\times 26,000$ ; inset,  $\times 130,000$ .





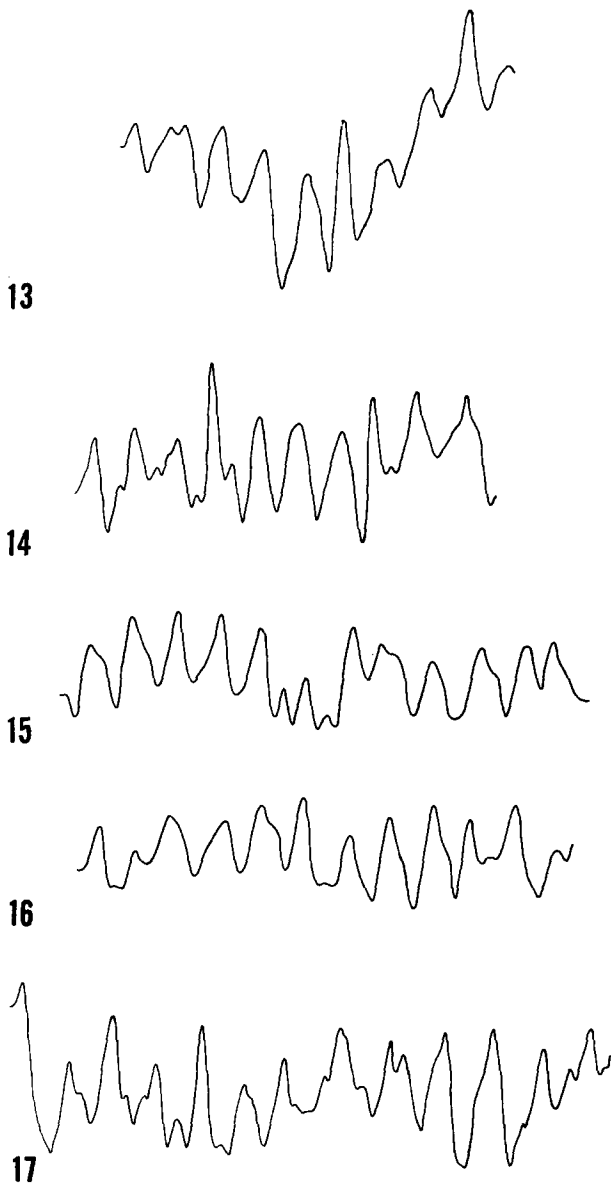


FIGURE 13 Microdensitometer tracing along the length of a vertically sectioned synaptic disc. The average period is 85 Å and is mainly due to the central beading. Lever ratio 100:1; slit width 1.0 mm.  $\times 610,000$ .

FIGURE 14 Microdensitometer tracing along the obliquely sectioned synaptic disc in the center of Fig. 9. Lever ratio 100:1; slit width 0.6 mm.  $\times 610,000$ .

FIGURE 15 Microdensitometer tracing along the obliquely sectioned synaptic disc in the inset to Fig. 10. The average period is 85 Å. Lever ratio 100:1; slit width 0.25 mm.  $\times 610,000$ .

FIGURE 16 Microdensitometer tracing along the obliquely sectioned synaptic disc in Fig. 11. The average period is 90 Å. Lever ratio 100:1; slit width 1.0 mm.  $\times 615,000$ .

FIGURE 17 Microdensitometer tracing across a part of the synaptic disc (*d*) in Fig. 18. The specimen was adjusted so that the slit was roughly parallel to the periodic lines that may be seen by tilting Fig. 18 and sighting along the short axis of the incomplete disc. The average spacing is 94 Å. Lever ratio 50:1; slit width 0.75 mm.  $\times 620,000$ .

whereas in others they appear to have five sides. In the obliquely sectioned disc to the lower right in Fig. 12 (arrow 2 and the lower inset enlargement) one can make out regions of transition from the subunit facets to the repeating linear pattern. In such regions it appears that the thicker dense

lines represent the aligned and overlapping edges of adjacent subunit facets. The thinner appearing intraperiod line seems to be produced by the overlapping and aligned central dense spots of adjacent subunit facets. As one would expect, the borders of the facets when seen in frontal view

FIGURE 12 Section of club ending with presynaptic axoplasm to the right. A synaptic disc (arrow 1 and upper inset) appears in frontal view. The region designated by arrow 2 is enlarged below and the one marked by arrow 3 to the left center.  $\times 51,000$ . Upper inset  $\times 150,000$ ; middle inset  $\times 110,000$ ; lower inset  $\times 130,000$ .

appear slightly thinner than they do when viewed obliquely or on edge where overlap effects occur. The central dense spots of the facets, however, appear slightly larger in frontal view than they do when viewed obliquely. The reason for this is not yet completely clear, but it is being studied further in models.

The major repeating lines in the hexagonal array made by the borders of the hexagonal facets can be seen best in the frontal sections by tilting the micrographs and sighting along the surface of the page. If this is done with Fig. 12 the lines appear in register six times during  $360^\circ$  of rotation. This six-fold symmetry is typical of hexagonal arrays. The pattern, however, is not a perfect one. The axes are bent in some directions. In some places it appears that the major axial lines bifurcate with the insertion of another row of facets. As mentioned above, from close examination of the original plates, it appears that the pattern may contain a few five-sided figures in a predominance of six-sided figures. This may be related to the imperfections observed in the lattice.

The above findings are summarized in Fig. 19. This shows in A, a diagram of a synaptic disc sectioned vertically. To the right, at higher magnification, in B, C, and D the appearances of the synaptic discs are shown as they are progressively tilted. Below in E the frontal view of a disc after a full  $90^\circ$  of tilt is shown. Note how the central dense spots of the subunit facets line up to give the intraperiod line in the partially tilted membranes. A few pentagonal facets have been introduced to produce imperfections in the lattice.

The imperfections in the lattice, if indeed due to the presence of a few pentagonal facets, is most interesting for this is a feature of the Buckminster-Fuller type geodesic architectural domes (4) in which steel rods bonded in six-sided and five-sided figures or facets are fitted together in an extended sheet-like array. Such a rigidly bonded sheet can be deformed into a spherical surface without buckling if about 5 per cent deformation of the bond angles is allowed, a figure that is not unreasonable for protein molecules. This general type of structure has already been noted in the surfaces of certain viruses (3, 4, 17, and 18) and it appears that the same kind of structural plan may be used in membranes if we assume that the presently described pattern does not represent an artifact, a matter than can only be decided by further work.

It appears from the micrographs that images of

the hexagonal patterns observed in frontal views of synaptic discs may be produced principally by some structural features mainly confined to the outer surfaces of the two unit membranes joined in the discs, for the beading in transverse sections is most definite in this location. However, one must consider the possibility that the pattern is produced by structural differentiations extending all the way through the synaptic disc unit membranes (*e.g.* the scalloping and vague transverse lines in Fig. 4). One way to decide this is to study stereoscopic electron micrographs. A consideration of Fig. 20 will illustrate this point. Two models were constructed from drilled  $\frac{1}{4}$  inch brass hexagonal stock, soldered together, and cut to two thicknesses. In one model the thickness is taken as  $\sim 30$  A to correspond to the core layer of a synaptic disc and representing only the united outer surface strata of two unit membranes. The other is five times thicker to correspond to the whole  $\sim 150$  A thickness of a synaptic disc. It represents two complete unit membranes united along their outside surfaces. These two models were soldered together and fixed to a supporting rod and a frame that allowed rotation of the composite model through  $360^\circ$ . The model was inserted into a photographic enlarger in the position normally occupied by a negative. The projected image was printed at various angles of tilt. Fig. 20 A shows it viewed edge-on (taken as  $90^\circ$ ). This corresponds to a transversely sectioned synaptic disc. F shows the model tilted to  $0^\circ$ , *i.e.*, to the horizontal position. This corresponds to the frontal views of synaptic discs. The other views show intermediate degrees of tilt. B is at  $81^\circ$  from the horizontal; C is at  $60^\circ$ ; D is at  $22^\circ$ ; E is at  $15^\circ$ . Note in B, at a very slight tilt from the vertical, the appearance of transverse periodic lines mimicking the electron microscope image of the slightly tilted synaptic discs. In C the internal hexagonal pattern is completely obscured in both models; it begins to appear in the thinner model in D and the thicker model in E. The thicker model can be tilted  $\pm 20^\circ$  from the horizontal without losing the pattern completely and the thinner model can be tilted  $\pm 57^\circ$  with similar results. The pattern is about half obscured in the thicker model with  $\pm 10^\circ$  of tilt whereas the thinner model is equally obscured only by  $\pm 36^\circ$  of tilt.

The models suggest that if a reproducible series of electron micrographs of synaptic discs is taken

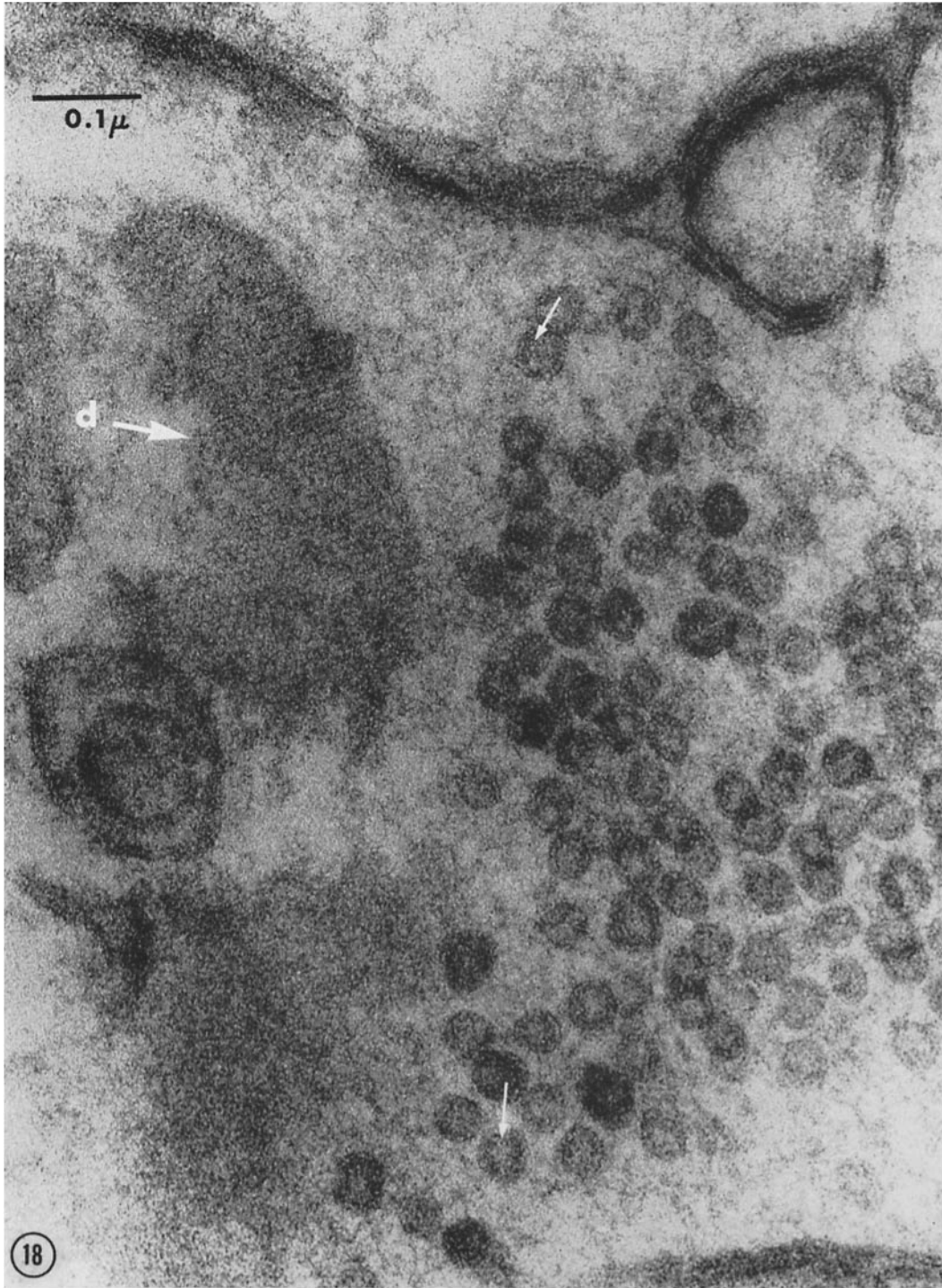


FIGURE 18 Section of synaptic disc (*d*) in frontal view with group of synaptic vesicles.  
× 160,000.

at the correct angles of tilt it should be possible to decide about the thickness of the elements responsible for the hexagonal pattern. A special stereoscopic specimen holder giving tilt angles of  $\pm 35^\circ$  for the Siemens Elmiskop has been constructed and preliminary experiments have been done. These seem to favor the thinner model but

ground of sections on carbon films. While the units in this pattern are not regularly arranged or of uniform size, some of them individually bear a close resemblance to the subunits in the membrane. This background pattern is apparently due to overlapping Fresnel fringes from small granules probably  $< 20 \text{ \AA}$  in diameter in the section or the

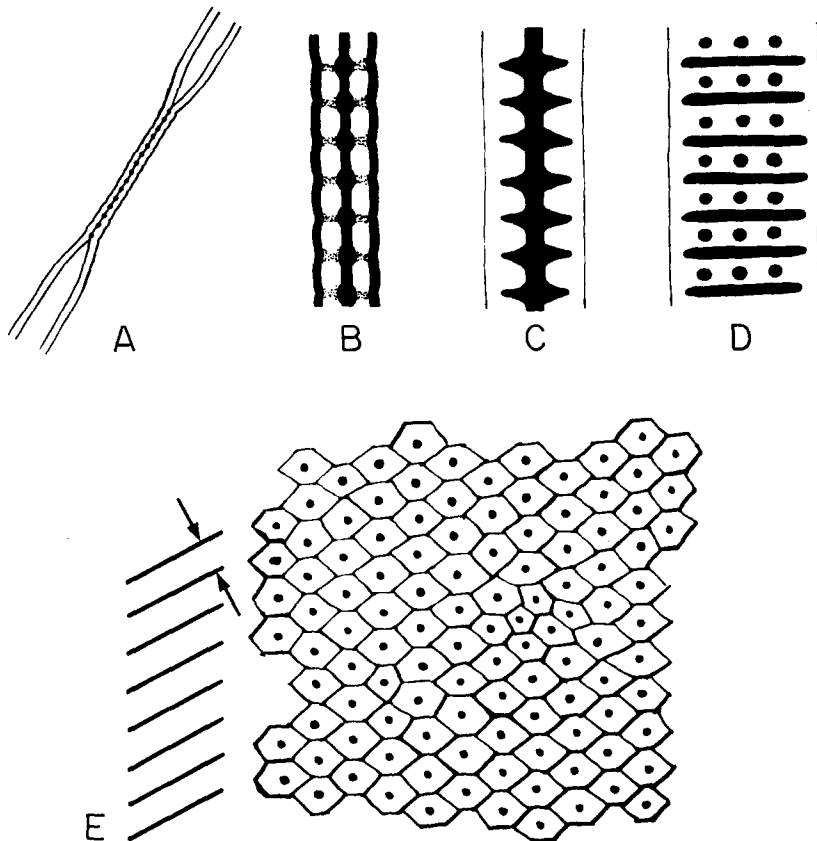


FIGURE 19 Diagrams of synaptic discs. A shows a synaptic disc with the adjacent SMC segments at medium power in vertical section. B shows a higher power view with more detail. Compare with Fig. 4. C shows the disc tilted slightly as the upper disc in Fig. 8. D shows a greater degree of tilt as in the top inset in Fig. 9 or the lower inset in Fig. 12. E shows a disc in frontal view as in the upper inset to Fig. 12. The main repeat period of  $\sim 95 \text{ \AA}$  is designated by the aligned arrows.

the results are still inconclusive mainly because of inadequate control of the specimen holder, but also because of rapid obscuration of the patterns by contamination. The method will be pursued and the results reported separately.

Although it does not show up clearly in the micrographs, it should be mentioned that an image pattern vaguely similar to that of the synaptic disc subunits appears in the general back-

supporting carbon film or both. It was necessary, particularly because of this background pattern, to do careful through-focus studies to eliminate the possibility that the image of the observed subunit pattern might be spurious. Such studies have shown that the background pattern drops out in micrographs close to exact focus while the honey-comb pattern of the synaptic discs does not. However, in such micrographs the contrast is

generally so low that the pattern in the synaptic discs, though definite on the original plates, is very difficult to reproduce in a photographic print. The pattern is best seen in such prints by sighting along the surface of the paper and rotating the page until one of the sets of periodic lines comes into register.

Figs. 21 to 24 and 25 to 28 show selected micrographs from two sets of through-focus series of

in current did it disappear completely. Fig. 22 was taken one medium step below focus in the same way. Fig. 23 was taken one medium step above focus as judged on the fluorescent screen by eye and this is, as seen in the micrograph, nearest to exact focus in accordance with previous experience in which the state of focus was checked by Fresnel fringes at the edge of a hole in the specimen. The pattern can best be made out in Fig.

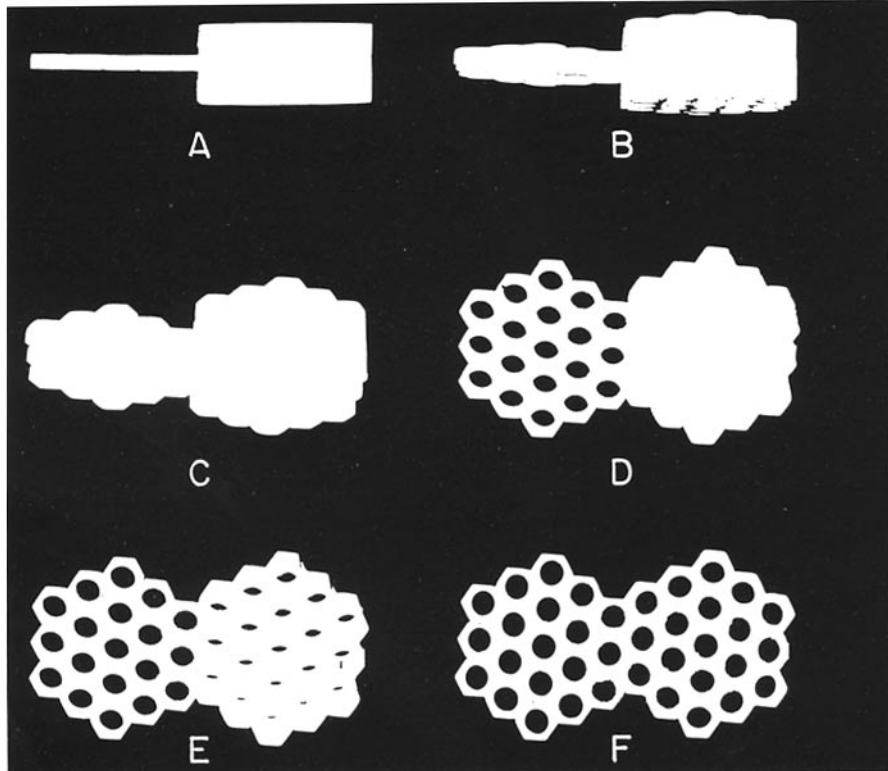
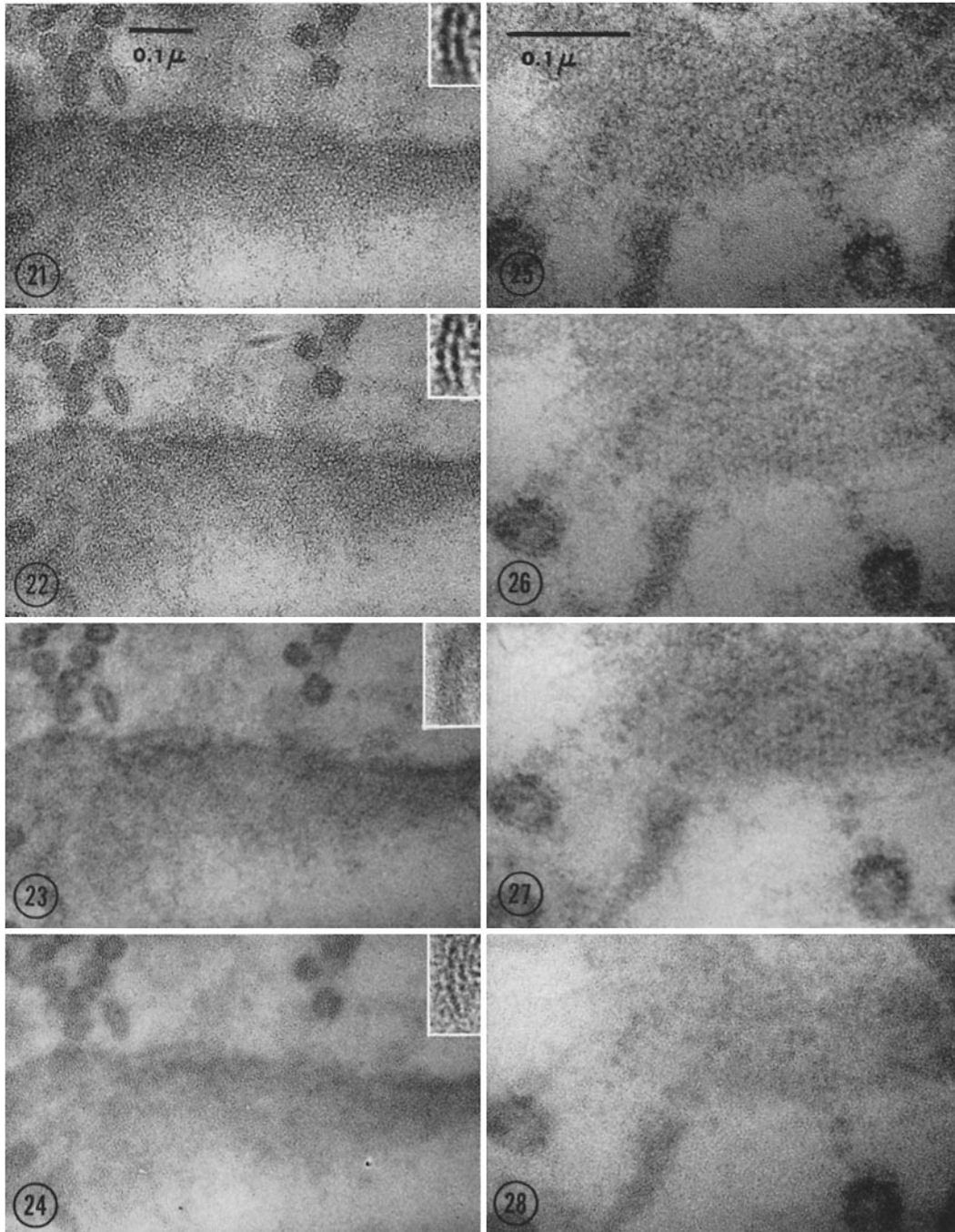


FIGURE 20 Composite model of two alternative structures for the hexagonal pattern in the synaptic discs. A shows the models in a vertical orientation. The thin model to the left represents a stratum  $\sim 30$  to  $40$  A thick. The attached thicker model represents a stratum  $\sim 150$  A thick. A is viewed at  $90^\circ$  from the horizontal; B at  $81^\circ$ ; C at  $60^\circ$ ; D at  $22^\circ$ ; E at  $15^\circ$ ; F at  $0^\circ$ .

synaptic discs in frontal views. Figs. 21 to 24 were taken at an electronic magnification of 40,000. The subunit pattern was brought into sharp focus on the fluorescent screen as judged visually with a Wray stereoviewer at  $\times 10$ . The image was then defocused by backing off two steps on the medium objective lens controller. Fig. 21 is thus considerably underfocused. However, the hexagonal pattern is still visible and only after further reduction

23 by sighting along the surface of the paper. The pattern could not be seen directly on the fluorescent screen at this state of focus because of its very low contrast but was visible in the photographic plate. Note the great reduction in background granularity as characteristically seen in exactly focused images. Fig. 24 was taken at two medium steps above exact focus. The background granularity is greatly increased and the regular



FIGURES 21 through 24 Through-focus series of frontal view of synaptic disc. The inset enlargement shows a transversely sectioned segment of a unit membrane from another area of the same plate in each micrograph.  $\times 89,000$ .

FIGURES 25 through 28 Another through-focus series of frontal view of a synaptic disc taken at a higher electronic magnification.  $\times 178,000$ .

pattern is not discernible. Although it is difficult to illustrate, a careful study of the micrographs shows that the distribution of light and dark spots in the image is reversed (*i.e.* dark spots in Figs. 21 to 23 are light spots in Fig. 24). The insets in Figs. 21 to 24 show a unit membrane from another area of these same micrographs. Note the reversal of the unit membrane pattern in the inset in Fig. 24. This is characteristic of grossly overfocused images of unit membranes as illustrated in another paper (27).

Figs. 25 to 28 show another through focus series taken at an electronic magnification of 80,000. In this case the correct image was first focused to maximum contrast on the fluorescent screen by eye. This was taken as an underfocused position because of previous experience using Fresnel fringes at an edge as a guide. The lens current was gradually increased in single steps with the fine focus controller as a succession of micrographs was taken until exact focus was reached and finally overfocused micrographs obtained. Fig. 25 is underfocused slightly. Fig. 26 was taken after an advance of four fine focus steps and is still underfocused. Fig. 27 was taken after two more fine steps (+6) and is closest to exact focus. Fig. 28 was taken after an advance of 14 fine focus steps from Fig. 25 and is distinctly overfocused. In Fig. 27 note that the background pattern due to fringes about grains that is so prominent in Fig. 25 virtually drops out but the hexagonal pattern in the synaptic disc is still faintly visible. At the next step in focus (Fig. 28) the background granularity rises sharply, the image reverses, and the subunit pattern disappears.

These through-focus studies seem to provide convincing evidence that the pattern observed in the synaptic discs is significant even though it is most clearly shown up in slightly underfocused micrographs. The pattern is destroyed by too intensive bombardment with the electron beam and also is fairly rapidly lost as contamination layers build up. It can be seen on the fluorescent screen at an electronic magnification of 20,000 with a 10 $\times$  stereoviewer using a pointed filament (6), a 100  $\mu$  condenser aperture, 50  $\mu$  objective aperture and a small beam diameter (+17 steps on condenser I controller). It is best seen at 80 to 100 kv. It must be searched for actively in several different endings and photographed rapidly. Often it is either not seen or disappears quickly before

it can be photographed. It was first seen on the fluorescent screen rather than in a micrograph.

An effort was made to increase the clarity of the display of the subunit patterns in frontal view by either taking the electron micrographs at higher electron microscope magnifications or enlarging the photographic plates to a greater degree. Neither of these procedures resulted in improvement. The pattern appeared regularly more clear in the lower magnification pictures. This was not the case for the synaptic discs in transverse section. The reason for this appears to be due to the image's being formed by somewhat punctate discontinuous structures. If these overlap sufficiently as in the transverse sections, higher magnification results in an apparent gain of detail; if they do not, as in the frontal sections, apparent detail is reduced by higher magnification. It is for this technical reason that the magnifications of all the frontal sections are relatively low.

It is important to decide whether or not the hexagonal facets seen in the united unit membranes of the synaptic discs occur in other unit membranes. While no such definite demonstration of the subunits has been made elsewhere suggestions of similar facets have been found in synaptic vesicles. In Fig. 12 the group of synaptic vesicles at arrow 3 is enlarged to the left center. These are unit membrane bounded spheres and the usual triple-layered pattern shows up where the membranes are viewed perpendicularly at the edges. Over the surfaces where the membranes are seen in frontal view at the top of the spherical vesicles there is a suggestion (arrows) of subunit facets like those seen in the synaptic discs. This point is somewhat more clearly made at the unlabeled arrows in Fig. 18 showing another synaptic disc (arrow *d*) and a group of synaptic vesicles in a club ending. Similar patterns have been found in the OsO<sub>4</sub>-fixed material. The possible appearance of the subunit facets in synaptic vesicles will be dealt with in detail in a separate paper.

The hexagonal pattern has been sought elsewhere. However, other tilted paired membranes have so far failed to show it convincingly. This should not necessarily be taken to mean that the pattern is not present elsewhere since a failure to demonstrate it could readily be due simply to technical specimen and instrumentation factors. For example, in other paired membranes there might be an absence of registration between patterns in adjacent membranes such as occurs in

the synaptic discs. This might obscure the pattern. For this reason it has been sought in tilted single unit membranes at the luminal borders of endothelial cells in brain capillaries. It has not so far been found. However, the failure could be due, if not to instrumentation difficulties, to the pattern's being too thin and delicate in a single membrane to give adequate contrast and withstand the electron beam. Suggestions of a similar pattern have been found in isolated fragments of  $\text{KMnO}_4$ -fixed membranes from other sources but the findings are too preliminary for inclusion here. At times suggestions of the pattern have been found in mitochondrial membranes, but this is so far not very convincing in our micrographs. Sjöstrand, however, has independently produced micrographs that seem to display a similar pattern in mitochondria (36). It thus appears that the pattern may have some general significance. Its demonstration in material fixed first in  $\text{OsO}_4$  as well as in material fixed first in  $\text{KMnO}_4$  operates against its being an artifact of permanganate fixation. However, it should be borne in mind that the  $\text{OsO}_4$  fixed specimens were postfixated or stained in  $\text{KMnO}_4$ .

#### DISCUSSION

With due consideration of the possibility that we could be dealing with some kind of fixation artifact, the findings reported here are tentatively interpreted to mean that the honey-comb appearance represents a direct derivative of a macromolecular pattern mainly localized in the outside lipoprotein or lipopolysaccharide-protein layer making the outer surfaces of unit membranes. The possibility must be entertained that the pattern extends all the way through the unit membranes as some micrographs might be taken to suggest. However, the slightest degree of tilt or wrinkling in the transversely sectioned synaptic discs could give such an effect even if the pattern is entirely confined to the central  $\sim 30$  to  $40$  A dense stratum. The scalloped appearance of the cytoplasmic dense stratum could also contribute to the effect. Another problem to be considered is whether or not the scalloped appearance and the vague transverse striations are indicative together of an altered physical chemical state of the membrane lipids as will be discussed further on.

A demanding question arises from the results as to whether or not a similar geodesic pattern could be present generally in unit membranes and yet have evaded until now clear demonstration.

Indeed, suggestions of regular repeating structures in the planes of unit membranes after various preparatory techniques have been obtained by others in the past. However, none of these resemble very closely the hexagonal pattern in the synaptic discs reported here. For example, Pease (24) has found a very regular pattern of dense beads repeating at a period of  $\sim 160$  A along two closely apposed outer mitochondrial membranes in a spherule of cat retina. He considered this dense beading to involve the whole of each of the two apposed unit membranes and he presented some evidence of dense bands running regularly through the cytoplasm from membrane to membrane at about the same period. He regarded this septate structure as comparable to the septate desmosomes described in hydra by Wood (39) and in earthworm giant nerve fibers by Hama (13). However, the latter structures involve only the *outer* dense strata of adjacent unit membranes rather than the inner, running, not through cytoplasm but through extracellular intermembrane gaps. Further, while the repeat period in Wood's micrographs is fairly close to that found by Pease, the one in Hama's micrographs is given as only  $\sim 60$  A.

Other references to structure within the plane of unit membranes have been made by Fernández-Morán (6) in retinal rod outer segments and Fernández-Morán and Finean (9) in myelin. These have involved granules  $< 50$  A in diameter repeating sporadically at intervals of well under  $75$  A and do not seem related to the presently reported pattern. Recently Fernández-Morán (6-8) has reported the occurrence of dense granules  $80$  to  $100$  A in diameter identified from correlated biochemical data (12) as "electron transport" or "elementary" particles in mitochondrial fragments. His findings have been confirmed by Parsons (23) and Stoeckenius (38). These particles appear to be attached to the matrix side of mitochondrial unit membranes by a narrow stalk and it appears that they are not integral constituents of the unit membranes themselves. Even if the subunit facets are present in mitochondria there is no obvious direct relationship between them and the electron transport particles; indeed, the two structures are related to opposite sides of the asymmetric unit membrane structure.

In the older literature Hillier and Hoffman (14) and Hoffman *et al.* (15, 16) observed a peculiar "plaque" structure in red blood cell ghosts dried down on a collodion film and shadowed with

metal. These plaques were  $\sim 100$  to  $500$  Å or more in diameter and were stated to be  $\sim 30$  Å thick. The great variability of these structures and their relatively large size makes it improbable that they are related to the subunit facets described in this paper. It seems quite reasonable to explain the plaque structure on dried red blood cells as a drying artifact rather like that appearing when mud dries in an empty pond bottom. There are, however, some difficulties with this explanation and it is conceivable that the plaques of Hillier and Hoffman are in some way related to the presently described subunit facets. The differences in dimensions, however, are so great as to make this unlikely.

Some time ago Gray (11) observed dense radial striae in myelin (see reference 29) that were subsequently shown by Peters (25) to be due to dense spots in successive intraperiod lines with the successive spots aligned radially. These dense spots were very much like those observed here in the synaptic discs in transverse views in that they occur in the outside surfaces of the unit membranes united at the intraperiod line and measure  $\sim 30$  to  $40$  Å in diameter. However, the spots were not found to repeat regularly along the plane of any individual intraperiod line in any spacing close to the ones reported here. Nevertheless, it may very well be that such regions in myelin are ones in which some kinds of subunits like those reported here are aligned in adjacent unit membranes. Their failure to appear elsewhere could be due to lack of alignment or equally well to an absence of any regular subunit pattern.

The recent findings of Dourmashkin *et al.* (5) are pertinent to the findings presented here. These investigators found a system of apparent holes about  $80$  Å in diameter in a regular hexagonal array with a repeating period of about  $160$  Å in presumed red blood cell membrane fragments. This was demonstrated by negative staining with phosphotungstic acid (3, 17) after treatment of the cells with B.D.H. (British Drug Houses) saponin. At first it appeared possible that some relationship might exist between the hexagonal pattern reported here and the pattern observed in saponin-treated membranes. However, the repeating periods are very different ( $\sim 85$  to  $95$  Å as compared to  $\sim 160$  Å). Furthermore, Bangham and Horne (1) and Glauert, Dingle, and Lucy (10) in Cambridge, England have independently found recently that pure cholesterol monolayers, when treated with saponin and formalin form a hex-

agonal lattice pattern just like the one found by Dourmashkin *et al.* This suggests strongly that the saponin treatment induces a molecular rearrangement in membranes whereby their cholesterol is extracted and deposited as complexes with saponin in a non-natural but regular arrangement. It would appear probable in this case that the very small sheet-like fragments identified as red blood cell membrane fragments by Dourmashkin *et al.* were sheets of complexes formed between saponin and lipids freed entirely from the native membrane itself and retaining none of the ordered structure of the native membrane. This argument cannot be applied directly in assessing the pictures reported here first, because the patterns reside in indubitable native membranes and secondly, because the same patterns appear after primary  $\text{OsO}_4$  fixation as well as primary permanganate fixation. Nevertheless, it is conceivable that permanganate might react selectively with some membrane components and cause them to rearrange in a regular pattern which is essentially an artifact. One would then have to suppose that the appearance of the pattern after primary  $\text{OsO}_4$  fixation followed by postfixation or "staining" with permanganate resulted from a reaction with membrane constituents not fixed by  $\text{OsO}_4$ . Although this appears unlikely, it should be considered. Experiments have been done in the past by the author in which monomolecular films of phospholipids were reacted with  $\text{KMnO}_4$ , embedded, and sectioned. No such hexagonal patterns as those shown here were demonstrated but the material will be examined again and the experiments repeated using negative staining methods.

The ever present problem of artifact that is almost as severe in fixed, embedded, and sectioned material as in isolated fractions restricts further interpretations of the findings until evidence from other technical approaches, such as the above, as well as further x-ray diffraction and polarized light studies of membranes can be obtained.

There is one final problem that requires further discussion. If the pattern observed in the synaptic discs exists in the native state it is conceivable that it is a manifestation of a local change in physical state of the membrane lipids from a layered smectic state such as that generally postulated for unit membranes to a cylindrical state of orientation such as Luzatti and Husson (20), and Stoeckenius (37) have demonstrated to exist in aqueous systems of certain extracted and purified lipids under certain conditions. This is favored by

the possibility that the pattern may occur only in localized regions in which highly restricted environmental factors might operate. In the membranes one might postulate the existence of a limiting state of the cylindrical system with the formation of lipid spheres within each unit membrane. This is an attractive interpretation for it would provide a means for establishing, reversibly, aqueous channels across the unit membranes. However, this seductive notion should not be accepted without very careful consideration of several points. First, if this interpretation is correct, one would expect the transverse striations in the membranes to be very distinct. Instead they are very faint and are explainable in other ways such as slight degrees of tilt or wrinkling of the membranes. Second, the postulated lipid spheres might be expected to be much smaller than the  $\sim 90$  Å figure indicated by the micrographs. Third, the unit membranes of the synaptic discs might be unusually susceptible to damage during fixation and the scalloped appearance, even if it is due to a change in state of the membrane lipids, might well represent an artifact. Fourth, there is some evidence that the subunit pattern may have more general significance. If this is so and the pattern is

associated with such a radical rearrangement of lipid molecules it is difficult to understand how previous investigators studying membranes by other biophysical methods such as polarization optical techniques and x-ray diffraction (see reference 29 for other references) could have failed to obtain some evidence for orientation of lipid molecules tangential to membrane surfaces. This objection does not apply, no matter how general the arrangement, if the structural differentiations are confined to the outer strata of the unit membranes for this kind of order could easily have been overlooked. For these reasons it is important to avoid premature conclusions and withhold judgment about any detailed molecular interpretation of the patterns observed until correlative evidence is forthcoming from other approaches to the problem.

The author is indebted to Miss Janet Lamborghini and Mrs. Ann Doughty for technical assistance and to Mr. Alfred Ley for photographic assistance. The work was supported by Grant B-2665 from the National Institutes of Health and a grant from the National Science Foundation.

Received for publication, March 19, 1963.

#### REFERENCES

1. BANGHAM, A. D., and HORNE, R. W., Action of saponin on biological cell membranes, *Nature*, 1962, **196**, 952.
2. BRADLEY, D. E., Simple methods of preparing pointed filaments for the electron microscope, *Nature*, 1961, **189**, 298.
3. BRENNER, S., and HORNE, R. W., A negative staining technique for high resolution electron microscopy of viruses, *Biochem. et Biophysica Acta*, 1959, **34**, 103.
4. CASPAR, D. L. D., and KLUG, A., Physical principles in the construction of regular viruses, *Cold Spring Harbor Symp. Quant. Biol.*, 1962, **27**, 1.
5. DOURMASHKIN, R. R., DOUGHERTY, R. M., and HARRIS, R. J. C., Electron microscopic observations on Rous sarcoma virus and cell membranes, *Nature*, 1962, **194**, 116.
6. FERNÁNDEZ-MORÁN, H., The fine structure of vertebrate and invertebrate photoreceptors as revealed by low-temperature electron microscopy, in *The Structure of the Eye*, (George K. Smelser, editor), New York, Academic Press, 1961, 521-556.
7. FERNÁNDEZ-MORÁN, H., Cell membrane ultrastructure: low-temperature electron microscopy and x-ray diffraction studies of lipoprotein components in lamellar systems, *Ultrastructure and Metabolism of the Nervous System*, Proc. of the Assoc. for Research in Nervous and Mental Disease, (S. R. Korey, A. Pope, and E. Robins, editors), Baltimore, Williams and Wilkins, 1962, 235.
8. FERNÁNDEZ-MORÁN, H., Subunit organization of mitochondrial membranes, *Science*, 1963, **140**, 381.
9. FERNÁNDEZ-MORÁN, H., and FINEAN, J. B., Electron microscope and low-angle X-Ray diffraction studies of the nerve myelin sheath, *J. Biophysic. and Biochem. Cytol.*, 1957, **3**, 725.
10. GLAUERT, A. M., DINGLE, J. T., and LUCY, J. A., Action of saponin on biological cell membranes, *Nature*, 1962, **196**, 953.
11. GRAY, E. G., personal communication.
12. GREEN, D. E., BLAIR, P. V., and ODA, T., Isolation and characterization of the unit of electron transfer in heart mitochondria, *Science*, 1963, **140**, 382.
13. HAMA, K., Some observations on the fine structure of the giant nerve fibers of the earthworm

- Eisemia foetida*, *J. Biophysic. and Biochem. Cytol.*, 1959, **6**, 61.
14. HILLIER, J., and HOFFMAN, J. F., On the ultrastructure of the plasma membrane as determined by the electron microscope, *J. Cell. and Comp. Physiol.*, 1953, **42**, 203.
  15. HOFFMAN, J. F., On the reproducibility in the observed ultrastructure of the normal mammalian red cell plasma membrane, *J. Cell. and Comp. Physiol.*, 1956, **47**, 261.
  16. HOFFMAN, J. F., WOLMAN, I. J., HILLIER, J., and PARPART, A. K., Ultrastructure of erythrocyte membranes in thalassemia major and minor, *Blood*, 1956, **11**, 946.
  17. HORNE, R. W. and WILDY, P., Recent studies on the fine structure of viruses by electron microscopy, using negative staining techniques, *Brit. Med. Bull.*, 1962, **18**, 199.
  18. HOYLE, L., HORNE, R. W., and WATERSON, A. P., The structure and composition of the myxoviruses, II. Components released from the influenza virus particle by ether, *Virology*, 1961, **13**, 448.
  19. KARNOVSKY, M. J., Simple methods for "staining with lead" at high pH in electron microscopy, *J. Cell Biol.*, 1961, **11**, 729.
  20. LUZZATI, V. and HUSSON, F., The structure of the liquid-crystalline phases of lipid-water systems, *J. Cell Biol.*, 1962, **12**, 207.
  21. PALAY, S. L., MCGREE-RUSSELL, S. M., GORDON, S. JR., and GRILLO, M. A., Fixation of neural tissues for electron microscopy by perfusion with solutions of osmium tetroxide, *J. Cell Biol.*, 1962, **12**, 385.
  22. PARSONS, D. F., A simple method for obtaining increased contrast in araldite section by using post-fixation staining of tissues with potassium permanganate, *J. Biophysic. and Biochem. Cytol.*, 1961, **11**, 492.
  23. PARSONS, D. F., Negative staining of thinly spread cells and associated virus, *J. Cell Biol.*, 1963, **16**, 62.
  24. PEASE, D. C., Demonstration of a highly ordered pattern upon a mitochondrial surface, *J. Cell Biol.*, 1962, **15**, 385.
  25. PETERS, A. Plasma membrane contacts in the central nervous system, *J. Anat.*, 1962, **96**, 237.
  26. ROBERTSON, J. D., New observations on the ultrastructure of the membranes of frog peripheral nerve fibers, *J. Biophysic. and Biochem. Cytol.*, 1957, **3**, 1043.
  27. ROBERTSON, J. D., Structural alterations in nerve fibers produced by hypotonic and hypertonic solutions, *J. Biophysic. and Biochem. Cytol.*, 1958, **4**, 349.
  28. ROBERTSON, J. D., The ultrastructure of cell membranes and their derivatives, *Biochem. Soc. Symp.*, 1959, **16**, 3.
  29. ROBERTSON, J. D., The molecular structure and contact relationships of cell membranes, *Progr. Biophysics and Biophysic. Chem.*, 1960, **10**, 343.
  30. ROBERTSON, J. D., Cell membranes and the origin of mitochondria, in *Regional Neurochemistry*, Proceedings of the 4th Neurochemical Symposium, (S. S. Kety and J. Elkes, editors), Oxford, Pergamon Press, 1961, 497.
  31. ROBERTSON, J. D., Ultrastructure of excitable membranes and the crayfish median-giant synapse, *Annals N. Y. Acad. Sci.*, 1961, **94**, 339.
  32. ROBERTSON, J. D., A subunit pattern within the membranes of club endings and synaptic vesicles in Mauthner cell synapses, *Anat. Rec.* 1963, **145**, 276.
  33. ROBERTSON, J. D., BODENHEIMER, T. S., and STAGE, D. E. An electron microscope study of the Mauthner cell, 2nd annual meeting of the Society for Cell Biology, Francisco, 1962, 154, abstracts.
  34. ROBERTSON, J. D., BODENHEIMER, T. S., and STAGE, D. E., The ultrastructure of Mauthner cell synapses and nodes in goldfish brains, *J. Cell Biol.*, 1963, **19**, 159.
  35. ROSENBLUTH, J., and PALAY, S. L., The fine structure of nerve cell bodies and their myelin sheaths in the eighth nerve of the goldfish, *J. Biophysic. and Biochem. Cytol.*, 1961, **9**, 853.
  36. SJÖSTRAND, F. S., personal communication.
  37. STOECKENIUS, W., Some electron microscopical observations on liquid crystalline phases in lipid-water systems, *J. Cell Biol.*, 1962, **12**, 221.
  38. STOECKENIUS, W., Some observations on negatively stained mitochondria, *J. Cell Biol.*, 1963, **17**, 443.
  39. WOOD, R. L., Intercellular attachment in the epithelium of hydra as revealed by electron microscopy, *J. Biophysic. and Biochem. Cytol.*, 1959, **6**, 343.